Supplementary Information

Solution-based fabrication of mechanically transformative materials for implantable applications

Xinxin Zhang,[1] Anwei Zhou,[2,4] Gaohua Hu,[3,5] Yanyan Li,[3,5] Kuikui Zhang,[3,5] Bing Liu,[1,*], Xinghai Ning,[3,4,*] and Desheng Kong[3,5,*]

[1]College of Mechanical and Electronic Engineering, Shandong University of Science and Technology, Qingdao 266590, China. Email: metrc@sdust.edu.cn

[2]School of Physics, Nanjing University, Nanjing 210093, China.

[3]College of Engineering and Applied Sciences and Jiangsu Key Laboratory of Artificial Functional Materials, Nanjing University, Nanjing 210046, China. E-mail: dskong@nju.edu.cn, xning@nju.edu.cn

[4]National Laboratory of Solid State Microstructures, Collaborative Innovation Centre of Advanced Microstructures, and Chemistry and Biomedicine Innovation Centre, Nanjing University, 210093, Nanjing, China.

[5]State Key Laboratory of Analytical Chemistry for Life Science, Nanjing University, Nanjing 210046, China.

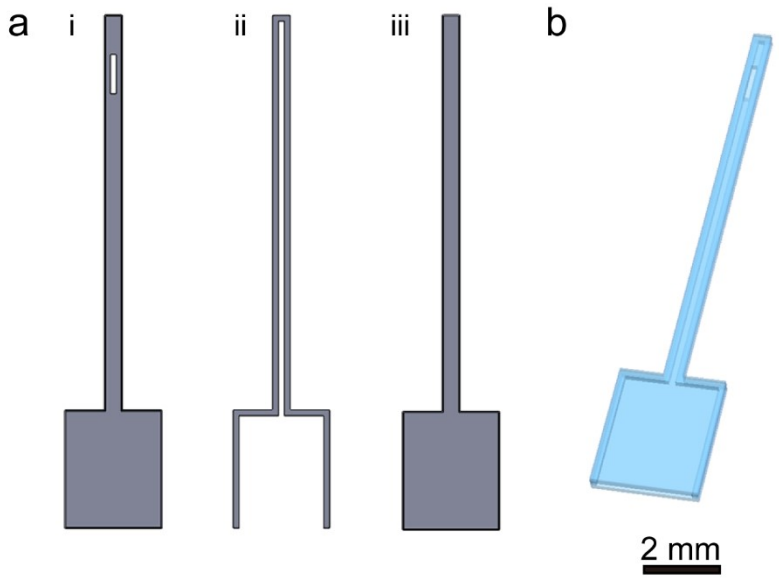

Figure S1. (a) Layer-by-layer patterns to generate the microfluidic channel for the mechanically transformative indwelling needle. Scar bar: (b) Schematic of the three-dimensional structure of the microfluidic channel. Notice that the opening is created on the side of the microfluidic channel to reduce the chance of blockage during implantation.

Figure S2. Optical image of a syringe barrel and indwelling needle assembly.

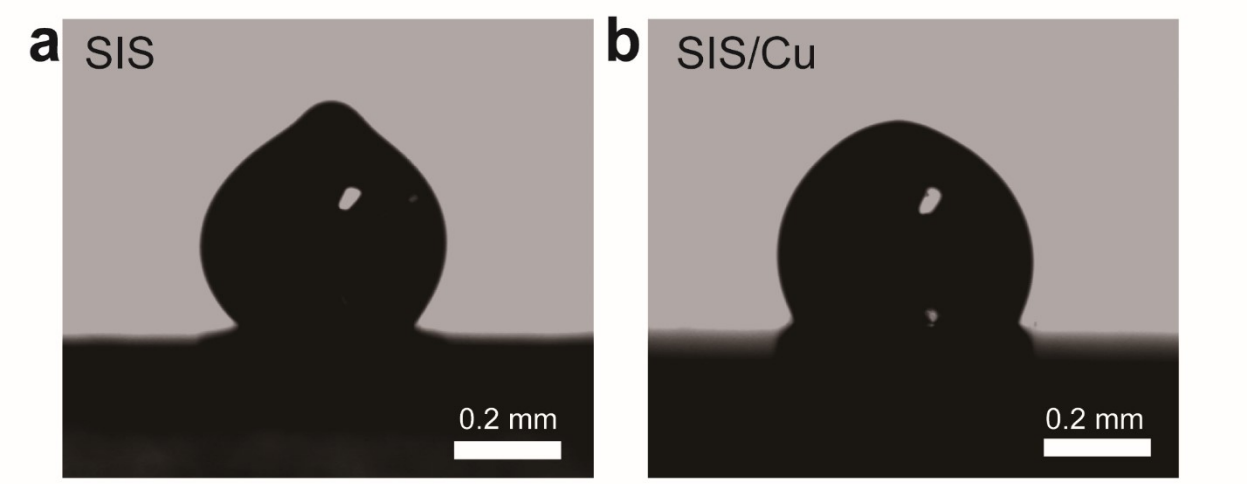

Figure S3. Contact angle images of Ga droplets on the pristine (a) and Cu-coated (b) SIS substrates under the ambient conditions. The contact angles are 123 ± 2° on SIS substrate and 118 ± 1° on SIS/Cu substrate.

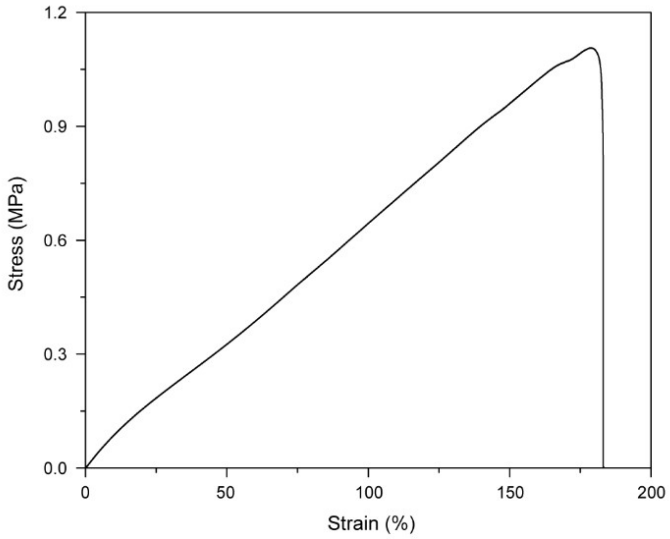

Figure S4. Stain-stress curve of the silicone elastomer (Dragon Skin 30) for encapsulation.

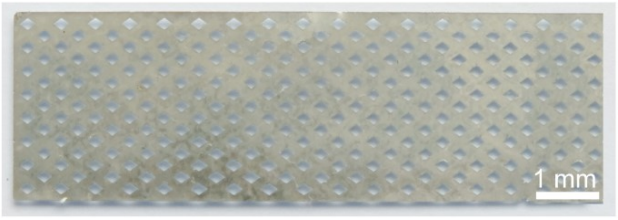

Figure S5. Optical image of a mechanically transformative mesh.

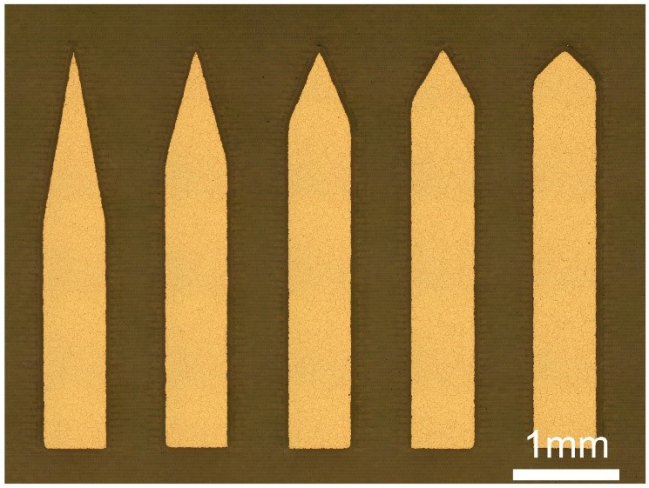

Figure S6. Optical microscopy image of Cu patterns with different tapering angles as the templates for Ga needles.

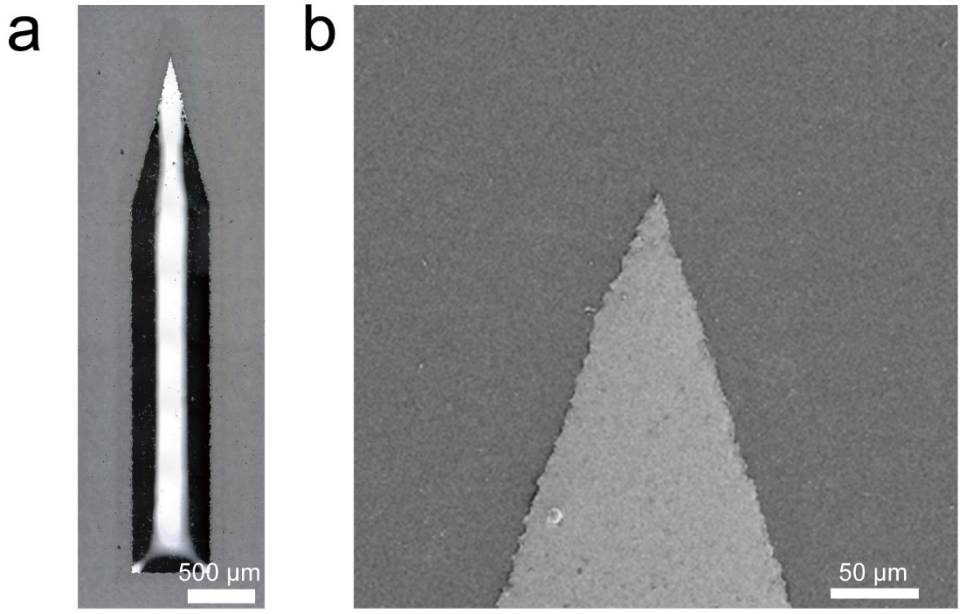

Figure S7. (a) Optical microscopy image of a representative Ga needle. (b) SEM image revealing a sharp needle with the tip size smaller than 5 μm.

Figure S8. Optical images of mechanically transformative indwelling needle before (left) and after (right) injection with red aqueous solution through the attached microfluidic channel.

Figure S9. Optical images of a mechanically transformative needle inserted into a skin phantom (1% agarose gel) at the stiff state (left) and manipulated at the soft states (middle and right). The skin phantom is maintained at ~40 ℃ on a hot plate. The needle has been thoroughly frozen before the implantation. The implanted fraction of the needle is switched into the soft state with negligible transfer of mechanical stress to the skin phantom under external manipulations.

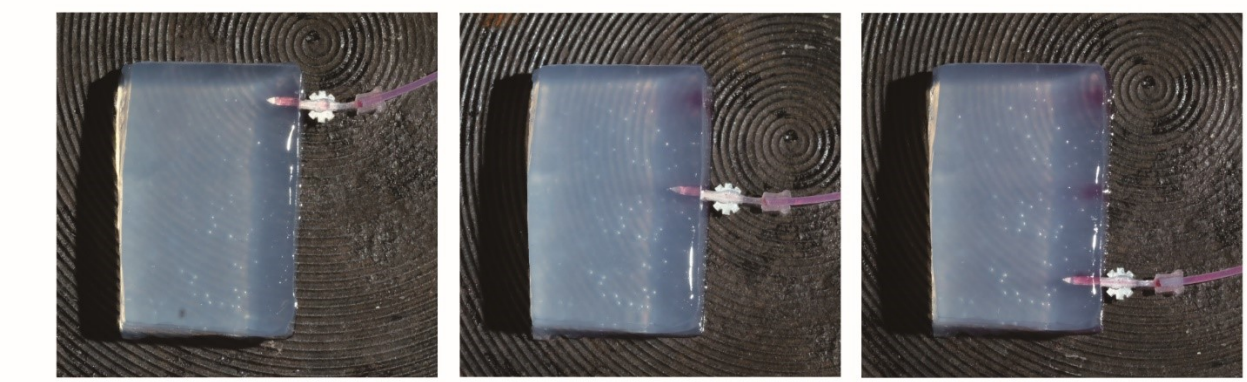

Figure S10. Multiple uses of the mechanically transformative indwelling needle. Optical images showing the injection of dyed aqueous solution into a skin phantom (1% agarose gel) by a mechanically transformative indwelling needle at three sites. The skin phantom is maintained at ~40 ℃ on a hot plate. The needle has been thoroughly frozen before each implantation. The implanted needle is easily pulled out at the soft state thanks to the elastomeric encapsulation.

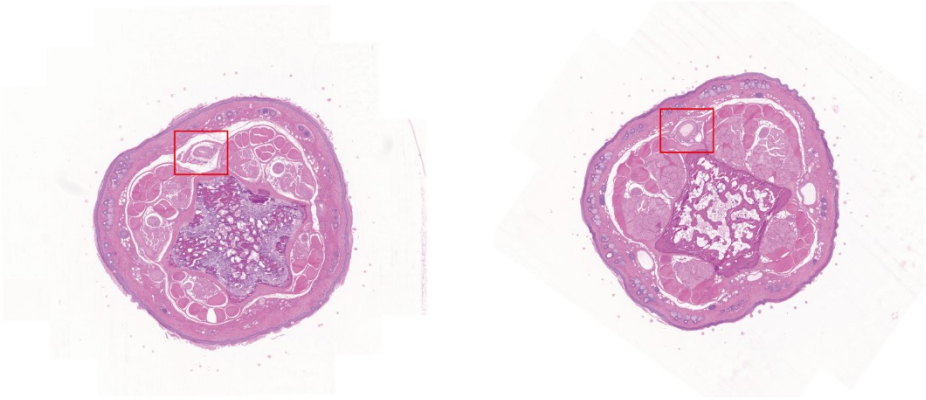

Figure S11. Hematoxylin-eosin (H&E) stained cross-sections of mouse tails prepared at 1 h (left) and 15 days (right) after the implantations of mechanically transformative indwelling needles.